Fungal Ecology 42 (2019) 100860

Contents lists available at ScienceDirect

Fungal Ecology

journal homepage: www.elsevier.com/locate/funeco

Local-scale spatial diversity patterns of ectomycorrhizal fungal communities in a subtropical pine-oak forest

Mayra E. Gavito [a, *], Ricardo Leyva-Morales [a], Ernesto V. Vega-Peña [a], Héctor Arita [a], Teele Jairus [b], Martti Vasar [b], Maarja Öpik [b]

[a] Instituto de Investigaciones en Ecosistemas y Sustentabilidad, Universidad Nacional Autónoma de México-campus Morelia, Apartado postal 27-3 Santa María de Guido, CP 58090, Morelia, Michoacán, Mexico
[b] University of Tartu, Department of Botany, 40 Lai street, 51005, Tartu, Estonia

ARTICLE INFO

Article history:
Received 26 October 2018
Received in revised form
3 August 2019
Accepted 6 August 2019
Available online 18 September 2019

Corresponding Editor: Marie Louise Davey

Keywords:
Distance-decay
Occupancy
Spatial autocorrelation
Similarity
species:area

ABSTRACT

This study aimed to analyze spatial patterns of soil ectomycorrhizal fungal (EMF) communities at the local scale in a subtropical pine-oak forest located in the Nearctic-Neotropical transition in central Mexico, to underpin biodiversity conservation strategies in forest fragments of this region. We used a spatially-explicit nested square sampling design with the same sampling representativeness at all scales and replicated three times. We detected 674 EMF OTUs within 19,200 m^2 and 65 OTUs on average per sample. Seventy percent of OTUs were detected in only 1–4 samples. Average community similarity was below 5%, showed minor change within 14 and 339 m distance and increased with the spatial grain used to compare the data. We found a high species-area relationship and beta diversity coefficients for soil fungi indicating that, at the local scale, increasing area by a constant factor of four represented an increase in OTU richness by a factor of two.

1. Introduction

Ectomycorrhizal fungi (EMF) form symbioses with plants mainly from the Betulaceae, Dipterocarpaceae, Fabaceae, Fagaceae, Pinaceae and Salicaceae (Brundrett, 2009). Their diversity is estimated to be high but is still largely unknown (Blackwell, 2011). There are few studies analyzing their spatial distribution patterns and drivers, and theses are mostly concentrated in temperate, Nearctic and Palearctic forests (Taylor, 2002; Bahram et al., 2013; Peay et al., 2016). EMF distribution patterns appear non-random and have been shown highly structured at local, regional and global scales (Bahram et al., 2014, 2016), and both horizontally and vertically at small, local scales, with large changes in species composition between samples taken only a few centimeters and meters apart (Tedersoo et al., 2003; Lilleskov et al., 2004; Izzo et al., 2005).

Soil fungi show high endemism when examined across a gradient of spatial scales, since the proportion of unique OTUs is maintained from the sampling point centimeter scale to the entire North America region (Talbot et al., 2014). EMF are nevertheless restricted, as obligate symbionts, to environments where host trees are present. Although their host species may have wide distribution ranges, forests with EM host trees are usually found in patches of different sizes in most current landscapes, making dispersal limitation and local environmental conditions particularly relevant for EMF distribution (Peay et al., 2012). A single ectomycorrhizal tree can host hundreds of fungal species (Bahram et al., 2011) that develop their external mycelium up to several meters away into the organic and mineral layers of the surrounding soil, forage for other nutrients and water and disperse depending on their morpho-functional traits (Hobbie and Agerer, 2010; Peay et al., 2011, 2012). At the local scale, although attached to the same host, EMF may thus encounter a variety of micro-environmental conditions that affect their development. EMF species composition changes continuously in response to the dynamic changes in biotic and abiotic factors that occur in the environment and select the species growing better under each new condition (Koide et al., 2007).

Temperate forest habitat loss and fragmentation due to land-use change are intense in central Mexico, and particularly in regions where highly profitable crops, like avocado (*Persea americana*), are continuously expanding over forest areas with ideal properties for

* Corresponding author.
E-mail address: mgavito@cieco.unam.mx (M.E. Gavito).

https://doi.org/10.1016/j.funeco.2019.08.004
1754-5048/

plantations (Bravo- Espinosa et al., 2012). This comes in addition to climatic alterations that have been predicted to lead to the disappearance of several tree species from the region within this century (Sáenz-Romero et al., 2012; UK Met Office, 2013). To date there are no studies that document spatial and temporal diversity patterns for EMF as the basis for biodiversity conservation strategies and policy in this region. Since EMF are crucial for the establishment and maintenance of the forests' dominant tree species, this knowledge is urgently needed to design successful biodiversity conservation programs that are appropriate for the current highly fragmented landscapes. Steep slopes, rocks and creeks create areas of low accessibility for management practices and are commonly left undisturbed within plantations and agricultural fields or rangelands. The potential of those small forest fragments for diversity conservation of EMF, and consequently also for plant and other forest-associated biota, is still unexplored. Therefore, we conducted a study aimed at (1) exploring the spatial patterns of EMF diversity in a forest fragment to define the sampling effort, distance and area required for adequately capturing the EMF species diversity, and (2) explore the spatial diversity and distribution patterns of EMF that help generating the criteria to guide site selection, sampling and up-scaling strategy in future landscape level studies. We hypothesized that, being in an environmentally heterogeneous region and a biogeographical realm transition, the study site would have high diversity, species turnover and spatially structured EMF communities and therefore high conservation value despite being a fragment.

2. Materials and methods

2.1. Study site

The study was conducted in a 120 ha, private-owned, pine-oak forest fragment covering a low mountain within an avocado orchard region in the city limits of Uruapan, Michoacán, in central Mexico (19° 29′ 01.24″ N, 102° 00′ 22.50″ W). This subtropical area has a semi-warm subhumid, dry-winter highland (1800 masl) climate, 1200–1500 mm annual rainfall, 16–20 °C mean annual temperature, and predominantly Andosol soils, which make this region ideal for avocado plantations (Gutiérrez-Contreras et al., 2010). Since the 1970s, pressure to convert temperate forests to avocado orchards has increased steadily, accelerating the transformation of the original large forested area into a matrix of scattered small patches of plantations, agricultural and rangelands, and forest fragments (Bravo-Espinosa et al., 2012). Small fragments are usually under additional pressure for pine-resin extraction and understory grazing. The study site was chosen, because it has been preserved by the owners without management for at least 50 y and represents better the biotic and abiotic conditions of a forest. Given the steep slopes of the mountain, we selected the low part of the hillside facing South-East where the slope was moderate, with no cliffs, and allowed safe walking and sampling despite having small creeks. The sampling area contained 11 woody species, from which five are ectomycorrhizal: *Pinus pseudostrobus. Pinus ayacahuite, Quercus subspathulata, Quercus obtusata* and *Quercus laeta*. *Pinus pseudostrobus* (23–40%) and *P. ayacahuite* (11–16%) had the largest relative importance values (RIV) over the sampling area and *Q. subspathulata* (14%) was important only in the upper part. Other woody species not forming ectomycorrhizas with high RIV were *Garrya longifolia* (18%) in the lower part, and *Saurauia serrata* (14%) in the middle part.

2.2. Sampling design

We used a spatially explicit nested plot design containing four spatial scales, as suggested by Arita and Rodríguez (2002) (Fig. 1). The largest spatial scale is a 80 × 80 m plot ($A_0 = 6400\ m^2$) divided into three additional spatial scales: (i) 4 subplots of 40 × 40 m ($A_1 = 1600\ m^2$), (ii) 16 subplots of 20 × 20 m ($A_2 = 400\ m^2$), and (iv) 64 subplots of 10 × 10 m ($A_3 = 100\ m^2$). We sampled 32 of the 64 subplots following a checkerboard design that allowed us to scale up from A_3 to A_0 by a constant factor of four maintaining the same sampling representativeness across the four scales. This nested plot was replicated three times (S1, S2, S3) in a connected diagonal arrangement that made it possible to evaluate species accumulation and community similarity with small gradual increases in linear distance and area. The longest linear distance between samples was 332.3 m and the largest cumulative area represented was 57,600 m^2 (although sampling maintained the same representativeness only up to 6,400 m^2), when adding S1, S2, and S3 plots (Fig. 1).

We took a single soil sample from the center of each 100-m^2 subplot. After removing all organic layers we hammered a clean 5-cm diameter PVC tube down the first 10 cm of the mineral soil layer and placed the soil sample in a Ziploc bag. Samples were taken to the lab, air-dried for two days and then stored in tubes with silica gel until DNA extraction (Davison et al., 2012; Vasar et al., 2017). DNA was extracted from 5 g of dried soil using PowerMax Soil DNA extraction kit (MO BIO Laboratories, Inc. Carlsbad, CA, USA) according to Gazol et al. (2016). First, to increase DNA yield, bead solution tubes were shaken at a higher temperature (60 °C as suggested by the manufacturer) for 10 min at 100 rpm in a shaking incubator. Second, before adding the final elution buffer, the samples were allowed to dry for 10 min at room temperature under the fume hood. Fungal sequences were amplified from soil DNA extracts using the ITS2 region with forward primers fITS7 (TCGTCGGCAGCGTCAGATGTGTATAAGAGACAGGTGARTCATCGAATCTTTG), and gITS7 (TCGTCGGCAGCGTCAGATGTGTATAAGAGACAGGTGARTCATCGARTCTTTG), and reverse primer ITS4 (GTCTCGTGGGCTCGGAGATGTGTATAAGAGACAGTCCTCCGCTTATTGATATGC) containing Illumina forward and reverse primer adapters (underlined),

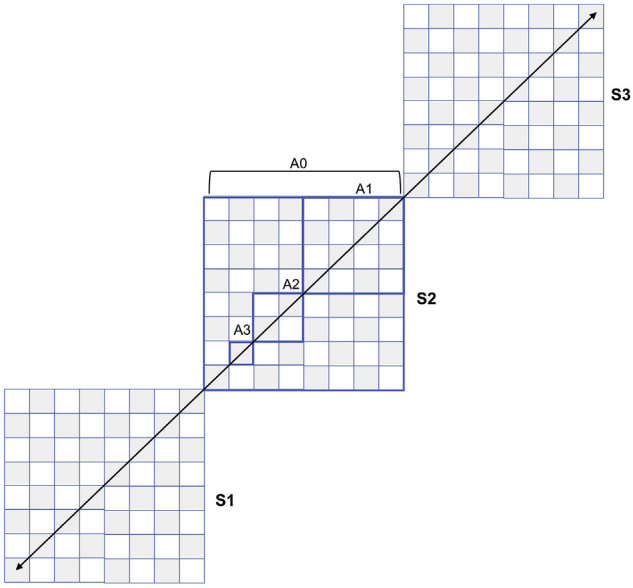

Fig. 1. Spatially explicit nested square sampling design. Spatial arrangement of the three 80 × 80 m replicate plots (S1-S3) showing the checkerboard sampling design and the four spatial scales ($A3 = 100\ m^2$, $A2 = 400\ m^2$, $A1 = 1600\ m^2$, $A0 = 6400\ m^2$) increasing with a constant factor of four. All shaded A3 squares were sampled in the center and linear distances between samples were calculated to the sampling point. The arrow shows the longest linear distance between two samples.

respectively, as suggested by Ihrmark et al. (2012) to amplify the fungal ITS2 region by targeting sites in the 5.8S encoding gene. PCR included two steps. The first PCR was performed in final volume of 30 μl with 3 μl of template DNA, 0.2 μM of each region-specific primer linked to partial Illumina sequencing adapters, and SmartTaq Hot Red 2× PCR Mix (Naxo OÜ, Estonia). The reactions were run on a Thermal Cycler 2720 (Applied Biosystems) with the program: 95 °C for 15 min, followed by 35 cycles of 95 °C for 30 s, 55 °C for 30 s, 72 °C for 30 s and ending with 72 °C for 7 min. PCR products were separated by electrophoresis through a 1.5% agarose gel in 0.5× TBE and purified first with the Qiagen QIAquick Gel Extraction kit (Qiagen Gmbh, Germany) and afterwards with the Agencourt® AMPure® XP PCR Purification system (Agencourt Bioscience Co., Beverly, MA, USA). The second PCR contained 5 μl of the purified product from the first PCR, Illumina Nextera XT Index kit primers to complete the sequencing adapters and add Nextera XT sample identifying indexes. The second PCR was made in the same volume and with the same conditions as the first PCR. The preparatory procedures for sequencing were performed by BiotaP LLC (Tallinn, Estonia). The resulting DNA library (250 ng) was sequenced using the Illumina MiSeq 2*300 v3 platform at Microsynth AG (Balgach, Switzerland).

2.3. Bioinformatic analyses

The sequence reads were examined and included in the analyses only if they contained the correct forward and reverse primer sequences for forward and reverse reads respectively. We obtained 2 x 21 685 263 paired-end sequences and processed them according to Gweon et al. (2015) using PIPITS v2.0. Briefly, the pipeline steps were 1) PIPITS_PREP: forward and reverse reads were combined with PEAR v0.9.8 (Zhang et al., 2014) and low quality reads were discarded if the average quality score over 80% of the sequence was under 30 using FASTX-Toolkit (Gordon and Hannon, 2010), 2) PIPITS_FUNITS: remaining sequences were extracted to match ITS2 subregion using profile hidden Markov models with ITSx v1.0.11 (Bengtsson-Palme et al., 2013), 3) PIPITS_PROCESS: extracted reads were dereplicated and clustered with 97% identity using VSEARCH v2.7.1 (Rognes et al., 2016) to produce operational taxonomic units (OTUs) 4) generated OTUs and members of the OTUs were subjected to chimera checking using VSEARCH in reference database mode against the UNITE database (v7.2, status December 2017, Kõljalg et al., 2005). and 5) taxonomic classification for each OTU was searched with RDP v2.7 (Deshpande et al., 2016) naïve Bayes classifier using UNITE database and a minimum boostrap value of 0.85. These processes obtained 18 226 423 combined reads, which were clustered into 10 378 fungal OTUs. Singletons were removed. OTUs are treated as species, with known limitations (Lindahl et al., 2013). The OTUs were further processed with the FUNGuild v1.1 software (Nguyen et al., 2015) to separate the ectomycorrhizal fungal species. Functional guild analysis allowed the assignment of 2572 OTUs to functional guilds. Sets of representative sequences of filtered paired-end Illumina from each OTU have been submitted to the EMBL nucleotide collection (accession numbers **LS420154-LS422775**).

2.4. Statistical analyses

All analyses were performed in R 3.5.0 (R Core Team, 2019) unless specified otherwise. We made rarefaction curves for the sequences recovered from each sample to identify low yield samples using the *rarecurve* function in the *vegan* package. Since only two samples rendered less than 1000 sequences, we kept them in the analysis to maintain the sampling representativeness of the experimental design (Fig. S1). All diversity and spatial analyses are presented with the entire data set without rarefying or normalizing the data because both procedures have some caveats. We considered it important to use all the information available for each sample given that rarefaction may exclude rare, but biologically relevant OTUs (Balint et al., 2016). We verified though that the spatial patterns observed with the full data set were the same as those obtained with data rarefied to the lowest sampling depth (575) using *rrarefy*. OTU richness and beta diversity were computed and are provided with the full data set and rarefied data, because the values differed, for comparison purposes. OTUs accumulation curves as a function of number of samples and Chao2 diversity estimator were calculated with EstimateS software (Colwell, 2013). We also constructed OTU accumulation curves as a function of linear distance and cumulative area with the *poolaccum* function of the *vegan* package. We used a linear regression model (*gam* function, *mgcv* package) to calculate the linear distance between sampling points from the starting point (100-m^2 subplot 1, Fig. 1) to the most distant (100-m^2 subplot 93, Fig. 1). The OTU accumulation curve as a function of increasing area was constructed by including the data from the 100-m^2 subplots enclosed after progressively increasing the size of the square by adding one column from the x axis and one row on the y axis until covering the total area of the three replicate plots (100, 400, 900, 1600, 2500, 3600, 4900, 6400 m^2). Afterwards the scale switched and the area expanded by including the data from the 6400-m^2 plots with gradual increases in x and y. At both scales the areas plotted include the enclosed areas that were not sampled. We used the collector accumulation method to add the linear distances or cumulative areas and used the predict function with the Michaelis-Menten model (as best-fit model) to calculate the predicted OTU accumulation until the curves approached an asymptote based on the observed data. We used the predicted values at that point to estimate completeness. We examined the frequency distribution of OTUs present in the 100-m^2 subplots as a measure of occupancy or range size within the S1-S3 plots and tested if the frequencies followed a normal distribution in the log scale with a Shapiro-Wilk normality test. Finally, we explored if the OTU frequencies correlated in the three plots.

We performed the spatial pattern analyses at the community level using the data from the sample taken at the center of each 100-m^2 subplot (A_3) as the sampling unit, unless specified otherwise. First, we explored whether community similarity between pairs of samples decreased with linear distance or with area using decay plots. We calculated similarity (1-Bray Curtis) with the Bray method using the *vegdist* function in the *vegan* package and calculated an Euclidean distance matrix for the linear distances between samples with Euclidean method using the *dist* function. Community similarity (1-BC) was plotted as a function of distance between samples and analyzed using a linear model and 1000 random permutations in stats. We examined and selected in all cases the best-fit and simplest model for the data. The similarity-distance relation was examined at the three area scales, 100, 400 and 1600 m^2 that allowed replication to examine the effect of the spatial grain used on the estimates of this relation. Finally, we plotted the mean similarity between all points at each area scale, selected a Michaelis-Menten model as the best-fit for these data and performed 1000 data permutations to examine the similarity-area relation.

To explore spatial autocorrelation, we used a Mantel correlogram (*mantel.correlog*, *vegan*) and a variogram (*variog*, *geoR*). The correlogram was calculated with the Euclidean distance matrix and the Bray method as explained before, grouping the data in 24 classes and with 1000 permutations. We assigned x, y coordinates to each sampling point with the *as.geodata* function (*geoR*) for the variogram and plotted a 95% confidence interval with the *envelope* function in *variosig*. Whittaker's beta diversity coefficients were

calculated as −log of the slope of the regression line obtained from the log OTU richness vs area scale plot (Arita and Rodríguez, 2002) and *z*-values as the slope of the regression line of the $\log_{10}$ species-$\log_{10}$ area plot.

3. Results

We found 674 OTUs of ectomycorrhizal fungi (Table S1) comprising 2 730 797 sequences in total. The three plots had very similar basic composition Basidiomycota (83%), Ascomycota (13−14%) and Zygomycota (2−3%) in 61 EMF genera, with predominance of *Inocybe*, *Tomentella*, *Russula* and *Sebacina* species (Fig. S2). OTU accumulation curves, as a function of number of samples, revealed very similar curves for the three replicate plots (Fig. 2A). Sampling completeness based on Chao 2 was 74.3% for S1, 76.3% for S2, 74.8% for S3, and 85% considering all samples. Mean OTU richness obtained with the complete data set was 493 in the 6,400 m^2 of the three replicate squares and, after rarefaction to the lowest sampling depth, completeness was very similar but mean OTU richness was estimated as 309. The OTU accumulation curves computed as a function of increasing linear distance between the samples showed a very high recovery of new species within the first 200 m in linear distance (Fig. 2B), and within the 6400-m^2 plots as a function of increasing area (Fig. 2C). Considering the entire distance range, community OTU richness completeness based on predicted species accumulation was 92%. The model for the OTU-area curve predicted a lower number of OTUs than the total observed in the entire area represented, therefore completeness was 100%. However, it is important to remark that the model fit was lower for the area curve since there were many more observations to build the predictions based on distance than based on area and sampling representativeness was not constant across the area scale. We also examined the OTU accumulation-area curve using only the scales that maintained the same sampling representativeness, but the last predicted values were still slightly below the observed data, and the model fit was lower ($R^2 = 0.84$). Therefore, we present the curve including more observed data although sampling representativeness varies and decreases substantially after 6400 m^2.

The frequency distribution of occupancy of EMF OTUs at the smallest spatial scale, that is the number of 100-m^2 subplots in which a given OTU is present, showed prevalence of OTUs that were found only in very few of the smallest squares and very few OTUs that were present in many squares (Fig. S3). Frequency of occupancy distributions were highly similar for the three replicate S1-S3 squares where approximately 40% of the OTUs were found in only 1 or 2 squares, and 50% in less than five squares. Additionally, tests for normality using log-transformed data showed that frequency distribution of occupancy did not follow a log-normal distribution within each replicate (S1 $p = 0.34$, S2 $p = 0.46$, S3 $p = 0.38$). There was also a high correlation of the frequency of occupancy of the OTUs in the three replicate squares: R(S1-S2) = 0.873, R(S1-S3) = 0.854, R(S2-S3) = 0.868, i.e. the OTUs with high frequency of occupancy in one square had also a high frequency of occupancy in the other two squares. When comparing the frequency of occupancy of OTUs at the largest (replicate square) spatial scale, nearly 50% of the total OTU richness was present in the three squares, 20% was present in two squares, and 30% in only one square. The large squares contained 10.6% (S1), 6.9% (S2), and 12.6% (S3) of unique OTUs from the total OTU richness.

EMF community similarity showed a weak relationship with spatial distance at all scales examined as the slopes of all regression lines of the observed data were highly significant and negative but with slope values close to zero and the slopes with 1000 permutations were also very low and not significant (Fig. 3). The initial similarity, that is the intercept of the decay lines as a measure of similarity between EMF communities at zero distance and indicator of initial beta diversity (Soininen et al., 2007; Bahram et al., 2013), was very low and changed depending on the scale, or spatial grain, used for the comparisons. The initial similarity values were,

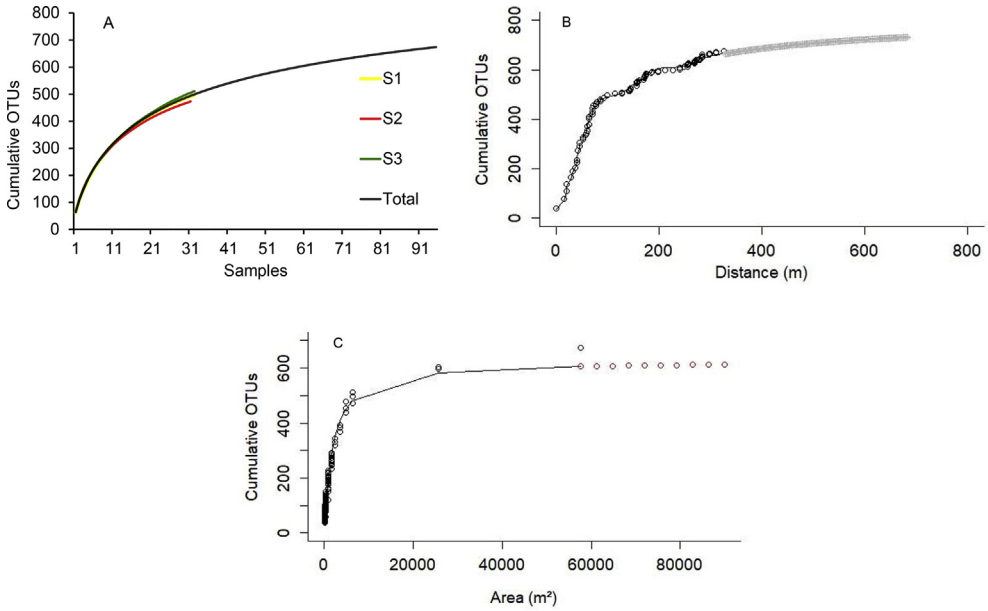

Fig. 2. Ectomycorrhizal fungal OTU accumulation curves. EMF OTU accumulation as a function of (A) sample numbers, showing the 32 samples collected from each of the three replicate plots and the 95 total samples, (B) increasing linear distance, considering the distance between samples from subplot 1 to all other subplots, and (C) increasing area, gradually expanding from subplot 1 to the complete square enclosing the three replicate plots (sampling representativeness is not maintained across scales in this figure). Empty circles connected by a line are the observed data and the grey line or circles after the line are the predicted data obtained with a random model and 100 permutations (R^2 distance = 0.98; R^2 area = 0.94).

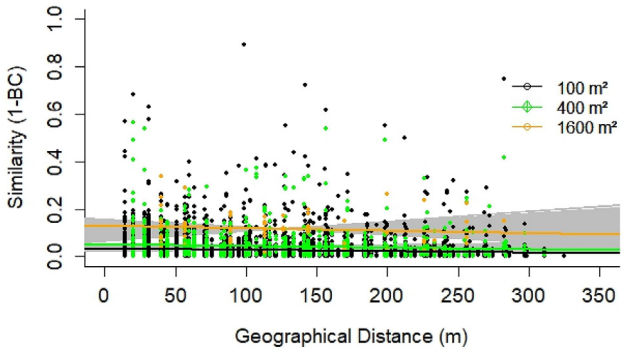

Fig. 3. Relationships between EMF community similarity (1-Bray Curtis dissimilarity index) and linear spatial distance. Similarity vs. distance relation between all sampling points compared using three spatial grains, 100 m^2 (black), 400 m^2 (green/dark grey) and 1600 m^2 (yellow/light grey). Solid lines are the regression lines for the observed data including all possible pair-wise comparisons at each spatial scale using data from the three replicate plots. (100 m^2) slope = - 4.8×10^{-5}, $p < 0.001$, $R^2 = 4.0 \times 10^{-3}$; (400 m^2) slope = -7.5×10^{-5}, $p < 0.001$, $R^2 = 6.5 \times 10^{-3}$; (1600 m^2) slope = -1.1×10^{-4}, $p = 0.351$, $R^2 = -1.8 \times 10^{-3}$). Overlapping light grey thin lines represent the regression lines for 1000 permutations: (100 m^2) slope = -6.0×10^{-5}, $p = 0.59$, $R^2 = -1.5 \times 10^{-4}$; (400 m^2) slope = 1.7×10^{-5}, $p = 0.50$, $R^2 = -4.9 \times 10^{-4}$; (1600 m^2) slope = 1.35×10^{-4}, $p = 0.24$, $R^2 = 0.5 \times 10^{-2}$).

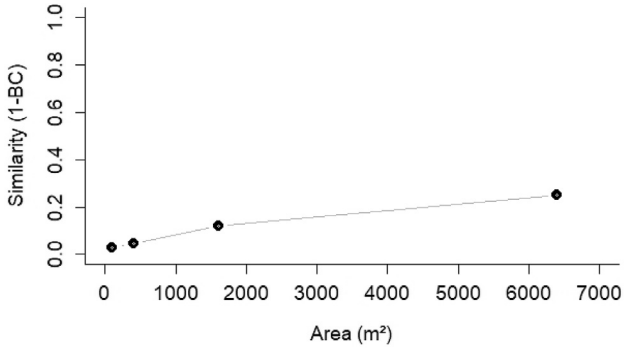

Fig. 4. Relationship between EMF community similarity (1-Bray Curtis dissimilarity index) and area. Similarity vs. area curve at four spatial scales, 100 m^2, 400 m^2, 1600 m^2, and 6400 m^2, using data from the three replicate plots. The points represent average similarity at each scale with the observed data and with 1000 permutations. The line shows the best-fit regression line using a Michaelis-Menten model fitted to all data including all pair-wise comparisons performed at each scale (intercept 0.0032, $p < 0.0001$; slope 0.5235, $p < 0.0001$; $R^2 = 0.9918$).

however, consistent with the observed data (100 $m^2 = 0.03$; 400 $m^2 = 0.05$; 1600 $m^2 = 0.13$) and the simulated data (100 $m^2 = 0.03$; 400 $m^2 = 0.04$; 1600 $m^2 = 0.10$). The slopes of the lines obtained with the permutation tests were also close to zero and not significant (Fig. 3). EMF community similarity increased with area (Fig. 4) (slope 0.5235, $p < 0.0001$) and the initial community similarity estimated was 0.0032 ($p < 0.0001$).

Both methods used to explore spatial autocorrelation, Mantel's correlogram and variogram, also suggested weak spatial autocorrelation (Fig. 5). Although there were four significant Mantel's test results indicating positive correlation between 10 and 60 m distance (Fig. 5A), the coefficients were close to zero and only one was highly significant (class 1, Spearman $r = 0.025$, $p < 0.03$; class 2, $r = 0.031$, $p < 0.03$; class 3, $r = 0.024$, $p = 0.049$; class 4, $r = 0.057$, $p < 0.004$). Those results are supported by the almost flat variogram (Fig. 5B).

OTU:area relationships were highly significant and showed a large spatial species turnover for EMF communities at the scales

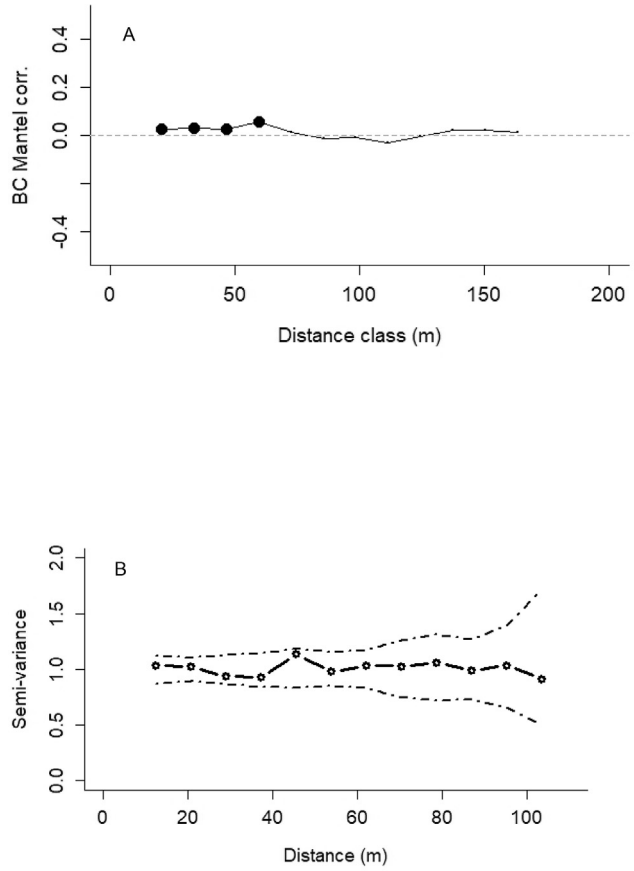

Fig. 5. Spatial autocorrelation tests. Mantel's correlogram (A) and variogram (B) for the ectomycorrhizal fungi communities at selected linear spatial distance classes. Black dots indicate distance classes with significant ($p < 0.05$, Bonferroni corrected) Mantel's r tests. Dashed lines show a 95% confidence interval in the variogram.

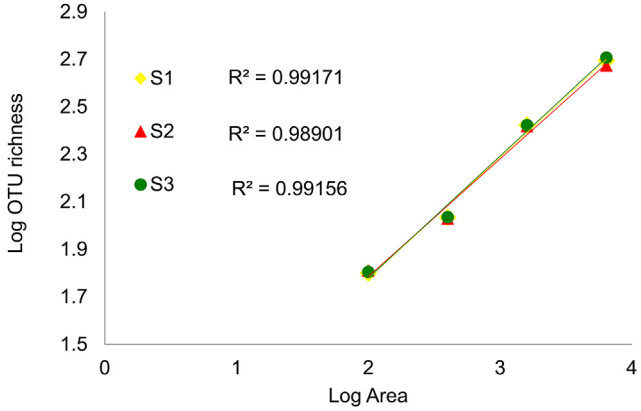

Fig. 6. OTU-area relationships. OTU richness-area (Log 10) regression lines for the three replicate plots at the four scales of measurement. S1 ($R^2 = 0.9917$), S2 ($R^2 = 0.9890$), S3 ($R^2 = 0.9916$).

measured (Fig. 6). Moreover, the regression lines obtained from the three replicate plots again showed strikingly similar spatial patterns and steep slopes at the three scales. OTU turnover was high, the *z*-values close to 0.5 (0.6 with rarefied data) and Whittaker β coefficients close to two (1.98–2.04 all data, 1.88 rarefied data) indicating that increasing area by a constant factor of four represented an increase in OTU richness by a factor of two (Table 1).

Table 1
OTU richness observed at four area scales. OTU richness and beta diversity coefficients, *z* and Whittaker's β, for the three replicate plots. Values used for regressions are the averages of OTU richness in 32 (100 m^2) subplots, the average cumulative richness in 16 (400 m^2) and 4 (1600 m^2) subplots, and the total OTU richness found in the 6400 m^2 S1-S3 plots. Averaged values are presented with standard deviations in parenthesis. *z* is the slope of the regression line of the log species-log area plot and β is -log of the slope of the regression line of the log species-area scale plot.

	Area (m^2)				Beta diversity	
	100 (A_3)	400 (A_2)	1600 (A_1)	6400 (A_0)	Z	β
S1	63 (15)	108 (19)	265 (29)	496	0.510	2.027
S2	64 (13)	107 (17)	262 (19)	472	0.495	1.986
S3	64 (12)	109 (17)	265 (7)	510	0.514	2.037

4. Discussion

Our study revealed a high spatial diversity and highly structured communities of ectomycorrhizal fungi (EMF) in the soil of this subtropical pine-oak forest. We found one of the highest reported OTU richness per unit area, OTU-area relationships and beta diversity coefficients for soil ectomycorrhizal fungal communities. Those results indicated that increasing area by a constant factor of four represented an increase in OTU richness by a factor of two within the scales studied. Moreover, the spatially explicit nested sampling design allowed us to recover strikingly similar spatial diversity patterns and OTU-area relationships from the three replicate plots. The 85% completeness for the 95 total samples based on Chao 2 estimates, 92% completeness based on cumulative distance projections and 100% completeness based on cumulative area, suggest an adequate sampling effort. The 32 samples, 113 m maximum linear distance, or 6,400 m^2 total area of a single replicate plot were clearly not reaching species saturation but all measures suggested nevertheless that including the three squares saturation was close, especially on an area basis. These results suggest that common sampling efforts including 10 independent samples, 50-m transects and sampling areas accumulating approximately 1000 m^2 found in the literature would likely be insufficient for an adequate representation of EMF diversity in this type of forest. Capturing 50–75% of the diversity in our study site would require more than 15 independent samples, 100 m distance or 5000 m^2 area sampling. However, these figures should be interpreted cautiously since next generation sequencing data have limitations and are highly influenced by bioinformatic processing decisions, particularly in terms of alpha diversity measures (Tedersoo et al., 2015; Barnes et al., 2016b; Vasar et al., 2017). Also, there are still few universally used approaches and statistical tools to determine sufficient sampling and appropriate data processing for sequences originating from study systems that may vary in complexity and therefore require different sampling intensities (Hart et al., 2015).

We found approximately 60 EMF OTUs on average (24 with rarefied data) per sample and an average of 493 (309, rarefied data) EMF OTUs in an equally-sampled cumulative area of 6,400 m^2, and with minimal variation between squares. The total richness is likely underestimated since 27% of the fungal OTUs could not be assigned to a named species and were thus excluded from the functional guild analysis. Although between-study alpha diversity comparisons must be interpreted with caution due to bias introduced by bioinformatic processing, the OTU richness values observed here (0.077 OTUs m^2 with all data, and 0.048 with rarefied data, within the 6,400 m^2 cumulative area of one square) are among the highest compiled by Bahram et al. (2015) for EMF at similar scales.

The highest values at similar scales reached 0.014 OTUs m^{-2} within 7,070 m^2 (Bahram et al., 2011) and 0.015 OTUs m^{-2} within 5,850 m^2 (Courty et al., 2008). They are also considerably higher than those reported by Talbot et al. (2014) for 25 Pinaceae-dominated forest sites across North America. Our figures for total and per-sample named and unidentified species, and beta diversity values (discussed below), are similar to those reported for root fungi in high-altitude Yungas forests in the Bolivian Andes (Barnes et al., 2016a). Such high richness was expected since the region is part of the Mexican transition zone, where the Nearctic and Neotropical biogeographical regions overlap, and is known to have high species richness and endemism for many taxa (Pinilla-Buitrago et al., 2018). The high biodiversity of this mountainous region has also been related to high environmental heterogeneity (Arita and Rodríguez, 2002) and environmental heterogeneity seems to play an important yet poorly understood role in EMF diversity and spatial distribution (Kennedy et al., 2012). The plots had a low diversity of EM hosts, two species of *Pinus* and three species of *Quercus*, but with high cover of those species over the sampling area (Leyva-Morales, unpublished results), and this agrees with previous observations of high EMF richness in tropical sites with high host tree density, but low host species richness (Peay et al., 2010; Tedersoo et al., 2010; Smith et al., 2011; Henkel et al., 2012).

The clear predominance of EMF OTUs showing restricted distributions to 1–2 sampling points, the consistency of OTUs being rare or common in the replicate squares, and the steep OTU-area relationships, provided strong evidence for no ubiquity and spatially structured communities at the local scale. We found slightly positive spatial autocorrelation in the Mantel correlogram between 20 m and 60 m distance and weak evidence for spatial autocorrelation from the variogram and distance-decay plots. This is likely related to the large distance between our sampling points since spatial autocorrelation is typically found at low distances, up to 2–3 m in temperate forests (Lilleskov et al., 2004), and extending to 10 m in tropical forests (Bahram et al., 2013). There may be correlation at smaller scales although those scales may vary widely, as seen in other studies performed in different sites (Bahram et al., 2015). Additionally, our data set has limitations in both spatial and temporal coverage that are important to fully understand diversity patterns (Barnes et al., 2016b) and should be addressed in future studies.

Our results contrast with Green et al. (2004) results for soil Ascomycota in Australia and Talbot et al. (2014) observations for soil fungi in North America, when compared within similar distances, since we found a minor decrease in similarity with increasing distance. When examined within a relatively small and homogeneous environment, similar to ours, Bahram et al. (2016) found positive spatial correlation for EMF within the first meters and mostly negative after 10 m distance. This pattern is common but can vary widely from site to site and within the distance ranges explored (Lilleskov et al., 2004).

Our analyses at different scales showed also that the scale of measurement influenced community similarity estimates and values at the largest scale were considerably higher than those found at the smaller scales. However, since initial community similarity was already below 5% from the beginning of the distance and area ranges, a steep decay could not be appreciated. Average similarity is often low in EMF communities (Bahram et al., 2013) and initial similarity is expected to be low at low latitudes (Soininen et al., 2007), but these values in our study were remarkably low. The large amount of data points to compare revealed consistently very low values and low dispersion in EMF community similarity. We believe this relation is maintained by a pool of a few generalist species that conforms the 1–20% average similarity and the rest of the community changes substantially from sample to sample. This explanation is supported by the high frequency of occupancy correlations of the most abundant OTUs in the three squares (same

generalists) and the high species turnover we found in the OTU-area and OTU-distance relationships (constant addition rate of new OTUs). The increase of community similarity with area, on the other hand, is likely due to a dilution of patchiness effects at larger areas. The overall patterns are likely due to a combination of likelihoods of EMF propagules dispersing to encounter a root to feed from and finding favorable environmental conditions to develop, that apparently go from very broad to very specific, and vary at a very small scale.

Our results are in accordance with published reports suggesting that, despite some distinguishable patterns suggesting greater distance-decay extent in the tropics (approx. 60 m) than in the non-tropics (approx. 20 m), distance-decay of community similarity seems highly site-specific (Lilleskov et al., 2004; Bahram et al., 2013). Spatially explicit sampling designs with replications and high representativeness allow for thorough examination of processes shaping biodiversity and, in this case, suggested weak spatial effects on EMF communities, as observed by Bahram et al. (2016) for soil microorganisms, and potentially stronger effects of stochastic processes to be examined in future studies.

We are also reporting one of the highest OTU-area relationships for microorganisms (Green and Bohanan, 2006; Bahram et al., 2016), fungi (Barnes et al., 2016a), and EMF (Peay et al., 2007; Bahram et al., 2016). Although comparisons ought to be cautious because of the differences in amplification and sequencing methods, species delimitation and bioinformatic processing that lead to different richness estimates, our data suggest a high richness of soil ectomycorrhizal fungi in our samples. This is an important finding that supports recent evidence (Argüelles-Moyao et al., 2016; García-Guzmán et al., 2017) indicating that the temperate forests in central Mexico harbor a large and unique biodiversity of EMF and should be preserved from the current human pressure exerted by land-use change and illegal logging (Navarrete et al., 2011; Bravo-Espinosa et al., 2012). Our results suggest that even moderate size forest fragments can maintain a high EMF diversity and that encouraging the conservation and connectivity of forest fragments within productive lands might succeed at preserving biodiversity, as suggested by Oliver et al. (2015).

Funding

RLM thanks Consejo Nacional de Ciencia y Tecnología (CONACyT) for a MSc scholarship and CONACyT and Programa de Apoyo a los Estudios de Posgrado of Universidad Nacional Autónoma de México (UNAM) for a research stay grant with Maarja Öpik at the Plant Ecology Lab of the University of Tartu, Estonia. MEG thanks financial support from UNAM-DGAPA-PASPA through a sabbatical scholarship and project UNAM-DGAPA-PAPIIT-IN203414 for financing research. MÖ, TJ and MV were funded by the Estonian Research Council (grant IUT20-28), the European Regional Development Fund (Centre of Excellence EcolChange) and ERA-NET Cofund BiodivERsA3 (Project SoilMan).

Acknowledgements

We thank Roberto Garibay Orijel and Diego Pérez Salicrup for their valuable suggestions, Guillermo Ibarra Manríquez and Guadalupe Cornejo Tenorio for tree species identification and Miguel Romero and Francisco Mora for help with the statistical analyses. The authors declare no conflict of interest.

Supplementary data

Supplementary data to this article can be found online at https://doi.org/10.1016/j.funeco.2019.08.004.

References

Argüelles-Moyao, A., Garibay-Orijel, R., Márquez-Valdelamar, L.M., Arellano-Torres, E., 2016. *Clavulina-Membranomyces* is the most important lineage within the highly diverse ectomycorrhizal fungal community of *Abies religiosa*. Mycorrhiza **27**, 53–65.

Arita, H.T., Rodríguez, P., 2002. Geographic range, turnover rate and the scaling of species diversity. Ecography 25, 541–550.

Bahram, M., Põlme, S., Kõljalg, U., Tedersoo, L., 2011. A single European aspen (*Populus tremula*) tree individual may potentially harbour dozens of *Cenococcum geophilum* ITS genotypes and hundreds of species of ectomycorrhizal fungi. FEMS Microbiol. Ecol. 75, 313–320.

Bahram, M., Kõljalg, U., Courty, P., Dhiédiou, A.G., Kjøller, R., Põlme, S., Ryberg, M., Veldre, V., Tedersoo, L., 2013. The distance decay of similarity in communities of ectomycorrhizal fungi in different ecosystems and scales. J. Ecol. 101, 1335–1344.

Bahram, M., Harend, H., Tedersoo, L., 2014. Network perspectives of ectomycorrhizal associations. Fungal Ecol. 7, 70–77.

Bahram, M., Peay, K.P., Tedersoo, L., 2015. Local-scale biogeography and spatio-temporal variability in communities of mycorrhizal fungi. New Phytol. 205, 1454–1463.

Bahram, M., Kohout, P., Anslan, S., Harand, H., Abarenkov, K., Tedersoo, L., 2016. Stochastic distribution of small soil eukaryotes resulting from high dispersal and drift in a local environment. ISME J. 10, 885–896.

Balint, M., Bahram, M., Eren, A.M., Faust, K., Fuhrman, J.A., Lindahl, B., O'Hara, R.O., Öpik, M., Sogin, M.L., Unterseher, M., Tedersoo, L., 2016. Millions of reads, thousands of taxa: microbial community structure and associations analyzed via marker genes. FEMS Microbiol. Rev. 40, 686–700.

Barnes, C.J., Maldonado, C., Frøslev, T.G., Antonelli, A., Rønsted, L., 2016a. Unexpectedly high beta-diversity of root associated fungal communities in the Bolivian Andes. Front. Microbiol. 7, 1377. https://doi.org/10.3389/fmicb.2016.01377.

Barnes, C.J., van der Gast, G.J., Burns, C.A., McNamara, N.P., Bending, G.D., 2016b. Temporally variable geographical distance effects contribute to the assembly of root-associated fungal communities. Front. Microbiol. B 7, 195. https://doi.org/10.3389/fmicb. 2016.00195.

Bengtsson-Palme, J., Ryberg, M., Hartmann, M., Branco, S., Wang, Z., Godhe, A., De-Wit, P., Sánchez-García, M., Ebersberger, I., de Souza, F., Amend, A., Jumponnen, A., Unterseher, M., Kristiansson, E., Abarenkov, K., Bertrand, Y.J.K., Sanli, K., Eriksson, K.M., Vik, U., Veldre, V., Nilsson, R.H., 2013. ITSx: improved software detection and extraction of ITS1 and ITS2 from ribosomal ITS sequences of fungi and other eukaryotes for use in environmental sequencing. Methods Ecol. Evol. 4, 914–919.

Blackwell, M., 2011. The fungi: 1, 2, 3 … 5.1 million species? Am. J. Bot. 98, 1–13.

Bravo-Espinosa, M.E., Mendoza, M., Carlón-Allende, T., Medina, L., Sáenz-reyes, J.T., Páez, R., 2012. Effects of converting forest to avocado orchards on topsoil properties in the trans-Mexican volcanic system, Mexico. Land Degrad. Dev. 25, 452–467.

Brundrett, M.C., 2009. Mycorrhizal associations and other means of nutrition of vascular plants: understanding the global diversity of host plants by resolving conflicting information and developing reliable means of diagnosis. Plant Soil 320, 37–77.

Colwell, R.K., 2013. EstimateS: Statistical Estimation of Species Richness and Shared Species from Samples. Version 9.0. http://purl.oclc.org/estimates.

Courty, P.E., Franc, A., Pierrat, J.C., Garbaye, J., 2008. Temporal changes in the ectomycorrhizal community in two soil horizons of a temperate oak forest. Appl. Environ. Microbiol. 74, 5792.

Davison, J., Öpik, M., Zobel, M., Vasar, M., Metsis, M., Moora, M., 2012. Communities of arbuscular mycorrhizal fungi detected in forest soil are spatially heterogeneous but do not vary throughout the growing season. PLoS One 7, 8.

Deshpande, V., Wang, Q., Greenfield, P., Charleston, M., Porras-Alfaro, A., Kuske, C.R., Cole, J.R., Midgley, D.J., Tran-Dinh, N., 2016. Fungal identification using a bayesian classifier and the 'warcup' training set of internal transcribed spacer sequences. Mycologia 108, 1–5.

García-Guzmán, O.L., Garibay-Orijel, R., Hernández, E., Arellano-Torres, E., Oyama, K., 2017. World-wide meta-analysis of *Quercus* forests ectomycorrhizal fungal diversity reveals south-western Mexico as a hotspot. Mycorrhiza 27, 811–822.

Gazol, A., Zobel, M., Cantero, J.J., Davison, J., Esler, K.J., Jairus, T., Öpik, M., Vassar, M., Moora, M., 2016. Impact of alien pines on local arbuscular mycorrhizal fungal communities – evidence from two continents. FEMS Microbiol. Ecol. 92, fiw073.

Gordon, A., Hannon, G., 2010. "Fastx-toolkit," FASTQ/A Shortreads Pre-processing Tools (Unpublished). http://hannonlab.cshl.edu/fastx_toolkit.

Green, J.L., Holmes, A.J., Westoby, M., Oliver, I., Briscoe, D., Dangerfield, M., Gillings, M., Beattie, A.J., 2004. Spatial scaling of microbial eukaryote diversity. Nature 432, 747–750.

Green, J., Bohannan, B.J.M., 2006. Spatial scaling of microbial biodiversity. Trends Ecol. Evol. 21, 501–507.

Gutiérrez-Contreras, M., Lara, B.N., Guillén, H., Chávez, A.T., 2010. Agroecología de la franja aguacatera en Michoacán, México. Interciencia 35, 647–653.

Gweon, H.S., Oliver, A., Taylor, J., Booth, T., Gibbs, M., Read, D.S., Griffiths, R.,

Schonrogge, K., 2015. PIPITS: an automated pipeline for analyses of fungal internal transcribed spacer sequences from the Illumina sequencing platform. Methods Ecol. Evol. 6, 973–980.
Hart, M.M., Aleklett, K., Chagnon, P.L., Egan, C., Ghignone, S., Helgason, T., Lekberg, I., Öpik, M., Pickles, B.I., Waller, L., 2015. Navigating the labyrinth: a guide to sequence-based, community ecology of arbuscular mycorrhizal fungi. New Phytol. 207, 235–247.
Henkel, T.W., Aime, M.C., Chin, M., Miller, S.L., Vilgalys, R., Smith, M.E., 2012. Ectomycorrhizal fungal sporocarp diversity and discovery of new taxa in *Dicymbe* monodominant forests of the Guiana Shield. Biodivers. Conserv. 21, 2195–2220.
Hobbie, E.A., Agerer, R., 2010. Nitrogen isotopes in ectomycorrhizal sporopcarps correspond to belowground exploration types. Plant Soil 327, 71–83.
Ihrmark, K., Bödeker, I., Cruz-Martinez, K., Friberg, H., Kubartova, A., Schenck, J., Strid, I., Stenlid, J., Brandström-Durling, M., Clemmensen, K.E., Lindahl, B.D., 2012. New primers to amplify the fungal ITS2 region – evaluation by 454-sequencing of artificial and natural communities. FEMS Microbiol. Ecol. 82, 666–677.
Izzo, A., Agbowo, J., Bruns, T.D., 2005. Detection of plot-level changes in ectomycorrhizal communities across years in an old-growth mixed-conifer forest. New Phytol. 166, 619–630.
Kennedy, P.G., Matheny, P.B., Ryberg, K.M., Henkel, T.W., Uehling, J.K., Smith, M.E., 2012. Scaling up: examining the macroecology of ectomycorrhizal fungi. Mol. Ecol. 21, 4151–4154.
Koide, R.T., Courty, P.E., Garbaye, J., 2007. Research perspectives on functional diversity in ectomycorrhizal fungi. New Phytol. 174, 240–243.
Kõljalg, U., Larsson, H., Abarenkov, K., Nilsson, R.H., Alexander, I.J., Eberhardt, U., Erland, S., Høiland, K., Kjøller, R., Larsson, E., Pennanen, T., Sen, R., Taylor, A.F.S., Tedersoo, L., Vrålstad, T., Ursing, B.M., 2005. UNITE: a database providing web-based methods for the molecular identification of ectomycorrhizal fungi. New Phytol. 166, 1063–1068.
Lilleskov, E.A., Bruns, T.D., Horton, T.R., Taylor,, D., Grogan, P., 2004. Detection of forest stand-level spatial structure in ectomycorrhizal fungal communities. FEMS Microbiol. Ecol. 49, 319–332.
Lindahl, B.D., Nilsson, R.H., Tedersoo, L., Abarenkov, K., Carlsen, T., Kjøller, R., Kõljalg, U., Pennanen, T., Rosendahl, S., Stenlid, J., Kauserud, H., 2013. Fungal community analysis by high-throughput sequencing of amplified markers - a user's guide. New Phytol. 199, 288–299.
Navarrete, J.L., Ramírez, M.I., Pérez-Salicrup, D.R., 2011. Logging within protected areas: spatial evaluation of the monarch butterfly biosphere reserve, Mexico. For. Ecol. Manag. 262, 646–654.
Nguyen, N.H., Song, Z., Bates, S.T., Branco, S., Tedersoo, L., Menke, J., Schilling, J.S., Kennedy, P.G., 2015. FUNGuild: an open annotation tool for parsing fungal community datasets by ecological guild. Fungal Ecol. 20, 241–248.
Oliver, T.H., Heard, M.S., Isaac, N.J., Roy, D.B., Procter, D., Eigenbrod, F., Freckleton, R., Hector, A., Orme, C.D.L., Petchey, O.L., Proença, V., Rafaelli, D., Suttle, K.B., Mace, G.M., Martín-López, B., Woodcock, B.A., Bullock, J.M., 2015. Biodiversity and resilience of ecosystem functions. TREE 30, 673–684.
Peay, K.G., Bruns, T.D., Kennedy, P.G., Bergemann, S.E., Garbelotto, M., 2007. A strong species-area relationship for eukaryotic soil microbes: island size matters for ectomycorrhizal fungi. Ecol. Lett. 10, 470–480.
Peay, K.G., Kennedy, P.G., Davies, S.J., Tan, S., Bruns, T.D., 2010. Potential link between plant and fungal distributions in a dipterocarp rainforest: community and phylogenetic structure of tropical ectomycorrhizal fungi across a plant and soil ecotone. New Phytol. 185, 529–542.
Peay, K.G., Bruns, T.D., Kennedy, P.G., 2011. Rethinking ectomycorrhizal succession: are root density and hyphal exploration types drivers of spatial and temporal zonation? Fungal Ecol. 4, 233–240.
Peay, K.G., Schubert, M.G., Nguyen, N.H., Bruns, T.D., 2012. Measuring ectomycorrhizal fungal dispersal: macroecological patterns driven by microscopic propagules. Mol. Ecol. 21, 4122–4136.
Peay, K.G., Kennedy, P.G., Talbot, J.M., 2016. Dimensions of biodiversity in the Earth mycobiome. Nat. Rev. Microbiol. 14, 434–447.
Pinilla-Buitrago, G.E., Escalante, T., Gutiérrez-Velázquez, A., Reyes-Castillo, P., Rojas-Soto, O.R., 2018. Areas of endemism persist through time: a palaeoclimatic analysis in the Mexican transition zone. J. Biogeogr. https://doi.org/10.1111/jbi.13172.
R Core Team R, 2019. A Language and Environment for Statistical Computing. R Foundation for Statistical Computing, Vienna, Austria. https://www.R-project.org/.
Rognes, T., Flouri, T., Nichols, B., Quince, C., Mahé, F., 2016. VSEARCH: a versatile open source tool for metagenomics. PeerJ 4, e2584.
Sáenz-Romero, C., Rehfeldt, G.E., Duval, P., Lindig-Cisneros, R., 2012. Abies religiosa habitat prediction in climate change scenarios and implications for monarch butterfly conservation in Mexico. For. Ecol. Manag. 275, 98–106.
Smith, M.E., Henkel, T.W., Aime, M.C., Fremier, A.K., Vilgalys, R., 2011. Ectomycorrhizal fungal diversity and community structure of three co-occurring leguminous canopy tree species in a Neotropical rainforest. New Phytol. 192, 699–712.
Soininen, J., McDonald, R., Hillebrand, H., 2007. The distance-decay of similarity in ecological communities. Ecography 30, 3–12.
Talbot, J.M., Bruns, T.D., Taylor, J.W., Smith, D.P., Branco, S., Glassman, S.I., Erlandson, S., Vilgalys, R., Liau, H., Smith, M.E., Peay, K.G., 2014. Endemism and functional convergence across the North American soil mycobiome. Proc. Natl. Acad. Sci. U.S.A. 111, 6341–6346.
Taylor, A.F.S., 2002. Fungal diversity in ectomycorrhizal communities: sampling effort and species detection. Plant Soil 244, 19–28.
Tedersoo, L., Hallenberg, N., Larsson, K.H., 2003. Fine scale distribution of ectomycorrhizal fungi and roots across substrate layers including coarse woody debris in a mixed forest. New Phytol. 159, 153–165.
Tedersoo, L., Sadam, A., Zambrano, M., Valencia, R., Bahram, M., 2010. Low diversity and high host preference of ectomycorrhizal fungi in Western Amazonia, a neotropical biodiversity hotspot. ISME J. 4, 465–471.
Tedersoo, L., Ramírez, K.S., Nilsson, R.H., Kaljuvee, A., Kõljalg, U., Abarenkov, K., 2015. Standardizing metadata and taxonomic identification in metabarcoding studies. Giga Sci 4, 34.
UK Met Office, 2013. Climate: Observations, Projections and Impacts. Summary Factsheet Mexico. http://www.metoffice.gov.uk/climatechange/policy-relevant/obs-projections-impacts.
Vasar, M., Andreson, R., Davison, J., Jairus, T., Moora, M., Remm, M., Young, J.P.W., Zobel, M., Öpik, M., 2017. Increased sequencing depth does not increase captured diversity of arbuscular mycorrhizal fungi. Mycorrhiza 27, 761–773.
Zhang, J., Kobert, K., Flouri, T., Stamatakis, A., 2014. PEAR: a fast and accurate Illumina Paired-End reAd mergeR. Bioinformatics 30, 614–620.